# Atomic Wave-Function Imaging via Optical Coherence

C. Schnurr, T. A. Savard, L. J. Wang,[†] and J. E. Thomas
*Physics Department, Duke University, Durham, North Carolina 27708-0305*
(Received 21 June 1994)

We demonstrate optical methods for studying the slowly varying part of atomic center of mass wave functions, i.e., with thermal plane-wave factors removed. Utilizing continuous spatial photon echo fields and a simple lens system, the techniques determine the spatial distribution of the slowly varying wave function when the echo field is measured in the image plane. The corresponding momentum space distribution is obtained with high momentum resolution (0.1% of the photon momentum) using Fourier transform optics.

PACS numbers: 42.50.Vk, 42.50.Md

Methods for manipulating atomic center of mass wave functions are being widely explored in the emerging field of atom optics [1,2]. A substantial part of this work involves the study of the interaction of atomic states with optical force fields. For precise characterization of optical forces, it is often necessary to achieve high momentum resolution (much less than the photon momentum), for example, in velocity selective coherent population trapping [3]. There is also substantial interest in methods for using atomic momentum distributions to characterize electromagnetic fields in cavities [4].

In this Letter, we demonstrate a technique which employs continuous spatial photon echoes [5] to study the slowly varying part of atomic center of mass wave functions, i.e., with thermal plane-wave factors removed, in both position and momentum space. We show that, within the paraxial approximation, the echo field in the image plane (Fig. 1) measures the spatial distribution of the atomic polarization which, in turn, determines the spatial distribution of the slowly varying wave functions. Similarly, using Fourier transform optics, the echo field in the Fourier plane yields the corresponding momentum space distributions. This technique achieves high momentum resolution ($10^{-3}$ photon momentum) because atomic momenta are measured relative to a photon recoil momentum rather than relative to a thermal atomic momentum as in previous atom deflection experiments [6].

The scheme of the wave-function imaging technique is depicted in Fig. 1. A beam of two-level atoms moving nominally in the **y** direction crosses two continuous preparation laser fields separated by a distance $y_{21}$. The first preparation region places the atoms in a superposition of the excited state $|e\rangle$ and the ground state $|g\rangle$ (Fig. 2), creating a macroscopic dipole moment. Because of the spread in Doppler shifts, the optical dipole moment dephases and the macroscopic coherent field radiated by the sample becomes negligible. On traversing the second preparation region, the atoms experience a $\pi$ pulse in their rest frame, which conjugates the accumulated phase shifts. Because of this conjugation, the atomic dipole moment rephases and a coherent echo field is generated downstream at a distance $y_{21}$ from the second preparation region. This continuous spatial photon echo is analogous to that normally obtained in the time domain [7]. The echo field propagates in the **z** direction through a lens which creates an image of the echo region. This image is observed using a detector array positioned to measure the spatial distribution of the atomic polarization. In addition, a portion of the echo field is reflected from a beam splitter and directed through a second lens. A detector array placed in the appropriate Fourier plane of this lens allows the momentum distribution of the atomic polarization to be observed.

The atomic polarization is sensitive to perturbations of the atomic wave functions near the rephasing point, since, in this region, the excited and ground state slowly varying wave functions have constant amplitudes and constant relative phase in the absence of external perturbations. Hence, the excited state wave function can be used as a

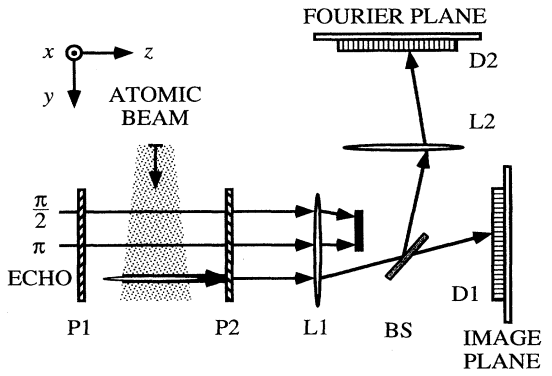


FIG. 1. Scheme of wave-function imaging. Atoms traverse two **x** polarized cw laser fields (polarized by $P1$). This creates a rephasing optical polarization downstream which radiates a coherent echo field. A **z** polarized light shifting beam (shown in white) propagates along **x** and is tightly focused along **y** onto the echo region. This beam creates a spatially varying potential for the atomic ground state. The echo signal passes through a **y** polarizer $P2$ and is imaged onto a diode array $D1$ in the image plane of lens $L1$. A part of the echo beam, reflected from a beam splitter BS, is Fourier transformed by lens $L2$ and observed in the Fourier plane with diode array $D2$. The image (Fourier) plane intensities reveal the ground atomic state position (momentum) distribution along **y**.

0031-9007/95/74(8)/1331(4)$06.00  

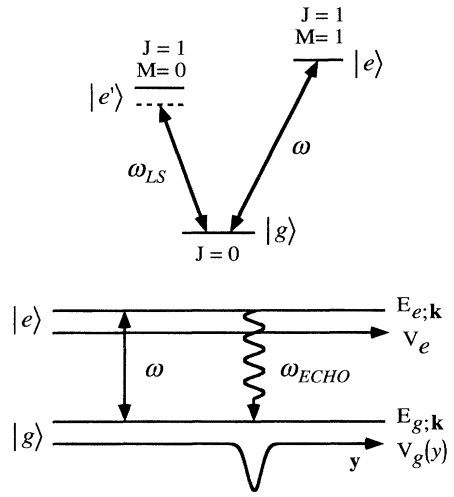


FIG. 2. Level diagram and an expanded view of the echo region with the light shift potential. A laser field of frequency $\omega$ excites the echo transition $|g\rangle \rightarrow |e\rangle$. An off-resonant light shifting beam ($\omega_{LS}$) interacts with levels $|g\rangle$ and $|e'\rangle$, creating an effective ground state potential $V_g(y)$. Since total energy is conserved, i.e., $E_{e,\mathbf{k}} = E_{g,\mathbf{k}} + \hbar\omega$, the coherently superposed states radiate an echo field at the frequency of the laser field $\omega$. The ground state momentum distribution along the **y** axis is altered by the potential.

reference wave for the ground state, enabling imaging of the slowly varying wave functions via the echo fields, as we now show.

For an atom with a center of mass velocity $\mathbf{v} \equiv \hbar\mathbf{k}/M$ prior to entering the preparation field regions, the wave function at position $\mathbf{R}$ can be written as

$$|\Psi_{\mathbf{k}}(\mathbf{R},t)\rangle = \frac{e^{i\mathbf{k}\cdot\mathbf{R}-iE_{g;\mathbf{k}}t/\hbar}}{\sqrt{V}}[\chi_{g;\mathbf{k}}(\mathbf{R},t)|g\rangle + \chi_{e;\mathbf{k}}(\mathbf{R},t)\,e^{i(qz-\omega t)}|e\rangle]. \quad (1)$$

$\chi_{g;\mathbf{k}}(\mathbf{R},t)$ and $\chi_{e;\mathbf{k}}(\mathbf{R},t)$ are the slowly varying center of mass wave functions of interest. It is assumed that the preparation fields of frequency $\omega$ propagate nominally along **z** with wave vector $q = \omega/c$. $E_{g;\mathbf{k}}$ is the sum of the ground state internal energy and the incident center of mass kinetic energy for the atom. For the superposition states which radiate the echo field, the total excited state energy differs from the ground state total energy by a photon energy $\hbar\omega$. Similarly, the excited state momentum differs from that of the ground state by a photon momentum $\hbar q$ along **z**. For this reason, $|\psi_{\mathbf{k}}(\mathbf{R},t)\rangle$ is expressed in the rotating frame where $\exp[i(qz - \omega t)]$ is factored out for the excited state.

The atomic polarization per unit volume is $\mathbf{P}(\mathbf{R},t) = N\langle\langle\Psi(\mathbf{R},t)|\hat{\mathbf{d}}|\Psi(\mathbf{R},t)\rangle_Q\rangle_{\mathbf{k}}$. $\langle\rangle_Q$ denotes the quantum average of the atomic dipole operator $\hat{\mathbf{d}}$ with respect to the internal atomic states, $N$ is the number of atoms in the quantization volume $V$, and $\langle\rangle_{\mathbf{k}}$ denotes a thermal average over initial atomic center of mass wave vectors. For continuous preparation fields and time independent external potentials, the atomic polarization can be written in the form $\mathbf{P}(\mathbf{R},t) = \mathrm{Re}\{\mathcal{P}(\mathbf{R})\exp[i(qz - i\omega t)]\}$, where $\mathcal{P}(\mathbf{R})$ is the slowly varying envelope of the polarization. For simplicity, we assume that $\mathcal{P}(\mathbf{R})$ varies only in the **y** direction, as is the case in our experiment. Then, Eq. (1) yields $\mathcal{P}(y) = 2n\mathbf{d}_{ge}\langle\chi_{e;\mathbf{k}}(y)\chi^*_{g;\mathbf{k}}(y)\rangle_{\mathbf{k}}$, where $n \equiv N/V$ is the atomic density. The echo field in the image plane is proportional to $\mathcal{P}(y)$ in the paraxial ray approximation, so that

$$\mathcal{E}_I(y) \propto \langle\chi_{e;\mathbf{k}}(y)\chi^*_{g;\mathbf{k}}(y)\rangle_{\mathbf{k}}\,. \quad (2)$$

Similarly, the echo field in the Fourier plane is

$$\mathcal{E}_F(p) \propto \int_{-\infty}^{\infty} dy\; e^{-ipy}\langle\chi_{e;\mathbf{k}}(y)\chi^*_{g;\mathbf{k}}(y)\rangle_{\mathbf{k}}\,, \quad (3)$$

where the momentum $\hbar p$ is related to position $y_f$ in the Fourier plane according to $p \equiv qy_f/z_f$. $z_f$ is the distance between the Fourier plane and the Fourier transform lens (Fig. 1) and $\hbar q$ is the incident photon momentum.

For an echo experiment with no external perturbing potentials, the product of the excited and ground state slowly varying wave functions near the rephasing point is approximately independent of velocity and slowly varying in space. In an ideal echo case, the first excitation is equivalent to a $\pi/2$ pulse in the atom frame, and the second excitation is equivalent to a $\pi$ pulse. Then, for $y > y_{21}$, $\chi^{(0)}_{g;\mathbf{k}}(y) \simeq (1/\sqrt{2})\exp[i(\phi_1 - \phi_2 - qv_z y_{21}/v_y)] \equiv \chi^{(0)}_{g;\mathbf{k}}$ is position independent. $\phi_i$ is the preparation field phase in region $i = 1, 2$, and the superscript (0) denotes the slowly varying wave function in the absence of a perturbing potential. Similarly, $\chi^{(0)}_{e;\mathbf{k}}(y) \simeq (i/\sqrt{2})\exp(i[\phi_2 - qv_z(y - y_{21})/v_y])$. With $y \simeq 2y_{21}$, the slowly varying polarization envelope is nearly independent of **v** and the dipoles rephase to radiate a strong, coherent echo signal. Near this rephasing point, $qv_z(y - 2y_{21})/v_y \ll 1$, and the product $\chi^{(0)}_{e;\mathbf{k}}\chi^{(0)*}_{g;\mathbf{k}}$ is approximately independent of position and velocity.

To demonstrate the imaging method, we modify the atomic ground state wave function using an off-resonant laser field which couples levels $|g\rangle$ and $|e'\rangle$ (Fig. 2). This provides a spatially varying light shift potential, $V_g(y)$, with a Gaussian profile. $V_g(y)$ affects only the ground state $|g\rangle$ of the echo transition. The corresponding Schrödinger equation is readily solved in this case by defining $\chi_{g;\mathbf{k}}(y) \equiv \chi^{(0)}_{g;\mathbf{k}}\,\psi_{g;\mathbf{k}}(y)$, where $\chi^{(0)}_{g;\mathbf{k}}$ is the amplitude given above for the $V_g(y) = 0$ case. Since $\chi^{(0)}_{g;\mathbf{k}}$ is position independent, $\psi_{g;\mathbf{k}}(y)$ is then the atomic ground state slowly varying wave function in the presence of $V_g(y)$. Hence, near the rephasing point, the image plane field is proportional to the average ground state slowly varying wave function, $\mathcal{E}_I(y) \propto \langle\psi_{g;\mathbf{k}}(y)\rangle_{\mathbf{k}}$. The field in the Fourier plane corresponds to the average ground state momentum space wave function, $\mathcal{E}_F(p) \propto \langle\psi_{g;\mathbf{k}}(p)\rangle_{\mathbf{k}}$. Thus, we say that the (average) slowly varying wave functions are "imaged." We note that for this method to be applicable the spatial coherence length of the atoms does not need to be longer than the length scale of the slowly

varying wave function. However, only in the long coherence length limit is $\psi_{g;\mathbf{k}}(\vec{R})$ the envelope of a true wave packet.

The atomic state $\psi_{g;\mathbf{k}}(y)$ does not vary significantly over the thermal velocity distribution ($\mathbf{k}$) for a supersonic atomic beam, as used in the experiments. Hence, the slowly varying wave functions of all atoms are approximately identical and $\psi_{g;\mathbf{k}}(y) \simeq \psi_g(y)$. Then, Eq. (2) shows that $\mathcal{E}_I(y) \propto \mathcal{E}_I^{(0)}(y)\psi_g^*(y)$, where the image plane field in the absence of $V_g(y)$ is $\mathcal{E}_I^{(0)}(y) = \langle \chi_{e;\mathbf{k}}^{(0)}(y)\chi_{g;\mathbf{k}}^{(0)*}\rangle_{\mathbf{k}}$. The spatial resolution in the image plane is limited in principle by diffraction due to finite lens apertures and in practice by the quality of the imaging system. The corresponding field in the Fourier plane is

$$\mathcal{E}_F(p) \propto \int_{-\infty}^{\infty} dy\ \mathcal{E}_I^{(0)}(y)\, e^{-ipy}\, \psi_g^*(y). \qquad (4)$$

The ground state momentum space wave function in the external potential is manifested in the distribution of momenta $p$. Using Fourier optics, the angle $\theta$ at which photons are emitted is measured. Since $\theta \equiv p/q = y_f/z_f$, the momentum $\hbar p$ in Eq. (4) is measured in units of the photon momentum $\hbar q$. Equation (4) also shows that the angular resolution is limited by the diffraction angle corresponding to the finite aperture of the echo rephasing region, i.e., the width of $\mathcal{E}_I^{(0)}(y)$ over which the field is coherent in the plane of the atomic beam. This diffraction angle is typically milliradians in the experiments. Hence, sensitivity to momentum transferred to the ground state by the spatially varying potential $V_g(y)$ and further, the accuracy of the ground state momentum-space wave-function measurement is at the milli-photon-momentum level as demonstrated below. It is interesting to note that momentum resolution in the Fourier plane is consistent with the uncertainty principle. This follows because the momentum space resolution is determined in the experiments by the Fourier transform of the finite aperture of the unperturbed echo field. Hence, the momentum resolution cannot be further improved by choice of lenses.

In the experiments, we use the $^7F_0, M = 0 \rightarrow {}^7D_1, M = 1$ transition in $^{152}$Sm at 599 nm, which has an excited state radiative lifetime of 1.7 $\mu$sec. Magnetic compensation of the Doppler shifts along $\mathbf{z}$ reduces the inhomogeneous linewidth of the medium, allowing the use of a relatively wide atomic beam ($\simeq$1 cm) [8]. Tremendous enhancement of the echo intensity is achieved with this method [5]. The $\mathbf{x}$ polarized preparation fields are blocked by observing the echo through a $\mathbf{y}$ polarizer. The intensity of the echo field is observed using a linear diode array with 25 $\mu$m spacing. In the image plane (magnification $-1$), the echo is approximately Gaussian with an intensity half-width at $1/e$ of $w_e \simeq 100$ $\mu$m.

The potential $V_g(y)$ is due to a Gaussian light shifting beam which propagates along $\mathbf{x}$ into the echo region from above. This beam is $\mathbf{z}$ polarized to access the $J = 0, M = 0 \rightarrow J = 1, M = 0$ transition (Fig. 2), thereby shifting only the ground state of the echo transition. The light shifting beam is 1.5 cm in diameter and is tightly focused with a cylindrical lens to an intensity half-width at $1/e$ of $w_s = 11$ $\mu$m along the atomic beam direction $\mathbf{y}$. The potential is approximately constant along the depth of the echo emission region, so that $V_g(y) \propto \exp[-y^2/w_s^2]$. The echo preparation beams are derived from the laser field which provides the light shifting beam by using a 110 MHz acousto-optic modulator to provide a fixed frequency offset. The laser frequency is stabilized so that the preparation beams are resonant with the $\Delta M = 1$ echo transition. The $M = 0$ and $M = 1$ excited states are split by an adjustable Zeeman field which places the light shift transition above or below resonance with the light shifting beam. The atomic beam is collimated in the vertical direction so that the Doppler shift of the light shifting beam is small compared to the detuning.

Figure 3 demonstrates the effects of the light shift potential on the momentum distribution of the echo field. The echo intensity $\propto |\mathcal{E}_F(p)|^2$ is detected with a diode array in the Fourier plane, $z_f = 0.45$ m from the transform lens. Figure 3(a) shows the results for an attractive perturbing potential, i.e., with the light shift beam detuned negatively. The unperturbed echo momentum distribution has an approximately Gaussian profile. With the potential applied, the momentum distribution of the echo field is

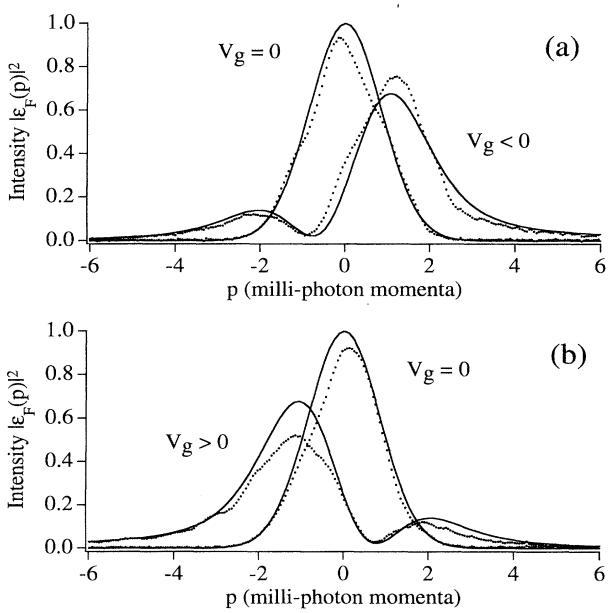


FIG. 3. Ground state momentum distributions measured as the echo intensity in the Fourier plane (dotted lines). Calculated ground state momentum distributions (solid lines). Data and calculated curves are normalized to the maximum echo intensity for the fit with $V_g = 0$ and plotted versus momentum $p$ along the $\mathbf{y}$ axis in units of $10^{-3}$ photon momenta. (Atomic source to the right.) (a) Attractive potential (negative detuning for the light shifting field); (b) repulsive potential (positive detuning for the light shifting field). Note that the momentum deflection due to the perturbing potential $V_g(y)$ is of order $10^{-3}$ photon momentum.

shifted toward the atomic source (to the left in Fig. 1), indicating that the atomic ground state mean momentum is increased, according to Eq. (4). Figure 3(b) shows the data for a positive detuning, i.e., a repulsive potential. In this case, the momentum distribution is shifted oppositely. In both cases, the momentum change is the order of a few milli photon momenta. It is also worth noting that the frequency of the echo field does not change as a result of the light shift. This is due to the fact that transitions occur between eigenstates of the total energy, Fig. 2.

The measured distributions can be compared to those calculated from the ground state slowly varying wave function. We use an eikonal approximation to the Schrödinger equation, which is appropriate because the potential energy $V_g(y)$ is small compared to the kinetic energy of the supersonic beam. In this case, $\psi_g(y) = \exp[-i\Phi(y - y_0)]$, where $\Phi(y) = (1/\hbar v_y)\int_{-\infty}^{y} dy' V_g(y')$ and $y_0$ is the displacement of the center of the light shifting beam from the center of the echo region. The echo field for $V_g(y) = 0$ is taken as $\mathcal{E}_I^{(0)}(y) = \exp[-(y/w_e)^2/2]$. The ground state phase shift can be written as $\Phi(y) = \phi_0 \int_{-\infty}^{y} dy' \exp[-(y'/w_s)^2]/w_s\sqrt{\pi}$, where $\phi_0$ is the phase shift acquired by a ground state atom which traverses the entire light shift region. This phase shift is measured experimentally by interfering the continuous free induction decay field from the $\pi/2$-preparation region with the echo field in the Fourier plane. The resulting interference pattern shows that the phase of the echo field does not appreciably vary across the echo aperture when $V_g(y) = 0$. By placing the light shifting beam between the $\pi$-preparation beam and the echo region, $\phi_0$ is determined as the phase shift of the fringes with and without the light shifting beam. For 135 mW of light shifting power and 45 MHz negative detuning (attractive potential), $\phi_0 = -2.2$ rad; for 45 MHz positive detuning (repulsive potential), $\phi_0 = +2.2$ rad. With an atomic velocity of 800 m/s, this corresponds to a depth of the attractive potential of 14 MHz. Calculated Fourier plane intensity distributions $|\mathcal{E}_F(p)|^2$ obtained from Eq. (4) are shown as the solid curves in Fig. 3. The experimental results are in excellent agreement with this simple model using the measured light shift potential parameters and the echo amplitude in the absence of the light shift potential. Note that for simplicity, we ignore the amplitude modulation due to the light shift beam. The offset $y_0$ of the light shifting beam from the echo center is adjusted to give the best fit to the data and is found to be 20 $\mu$m.

In conclusion, we have demonstrated the use of continuous photon echoes observed in the Fourier plane to measure the momentum distribution for the slowly varying wave function of a specific atomic state. Very high momentum resolution is achieved ($\approx 10^{-3}$ photon momentum). The experiments were done under conditions where all atoms have approximately identical spatial wave functions. In the general case, the atomic wave functions may not be nearly identical, and a proper statistical average is needed. Nevertheless, the method provides information about the momentum distribution of the states which are imaged. This method may have applications in studies of optical forces and in measurements of electromagnetic fields in cavities using atomic momentum distributions. Using homodyne detection, it is possible to measure the echo field, and hence obtain the phase and amplitude of the atomic slowly varying wave functions. The echo imaging method can be extended by employing Raman echoes [9,10], where coherence is stored in long-lived ground state sublevels and retrieved optically as in the present experiments. Such techniques may have unique applications in nonlinear optical processing and for information storage in ground state wave functions. Also, increased sensitivity to small potentials can be obtained by exploiting the method of weak measurement, as recently suggested theoretically [11] and subsequently demonstrated [12]. In this case, echoes on coupled transitions with different magnetic sublevels can be made to interfere. The echo intensity can be observed in a polarization rotation configuration, thereby greatly increasing the sensitivity to small optical forces which differently affect the superposed states.

This work has been supported in part by the Rome Air Development Center, the Air Force Office of Sponsored Research, the Army Research Office, and the National Science Foundation.

[†]Permanent address: Institute for Development of Advanced Technology, General Atomics, P.O. Box 85608, San Diego, CA 92186–9784.

[1] For an in depth review of atom optics, see C. S. Adams, M. Sigel, and J. Mlynek, Phys. Rep. **240**, 143 (1994).
[2] Special issue on atom optics, edited by J. Mlynek, V. Balykin, and P. Meystre, Appl. Phys. B **54** (1992).
[3] A. Aspect *et al.*, J. Opt. Soc. Am. B **6**, 2112 (1989).
[4] I. Sh. Averbukh, V. M. Akulin, and W. P. Schleich, Phys. Rev. Lett. **72**, 437 (1994); M. Freyberger and A. M. Herkommer, Phys. Rev. Lett. **72**, 1952 (1994).
[5] C. Schnurr, K. D. Stokes, G. R. Welch, and J. E. Thomas, Opt. Lett. **15**, 1997 (1990).
[6] P. J. Martin, P. L. Gould, B. G. Oldaker, A. H. Miklich, and D. E. Pritchard, Phys. Rev. A **36**, 2495 (1987).
[7] I. D. Abella, N. A. Kurnit, and S. R. Hartmann, Phys. Rev. **141**, 391 (1966).
[8] K. D. Stokes, C. Schnurr, J. Gardner, M. Marable, S. Shaw, M. Goforth, D. E. Holmgren, and J. E. Thomas, Opt. Lett. **14**, 1324 (1989).
[9] Multilevel photon echoes are described in T. W. Mossberg, R. Kachru, S. R. Hartmann, and A. M. Flusberg, Phys. Rev. **20**, 1976 (1979).
[10] R. Beach, S. R. Hartmann, and R. Friedberg, Phys. Rev. A **25**, 2658 (1982); R. Friedberg and S. R. Hartmann, Phys. Rev. A **48**, 1446 (1993).
[11] Y. Aharonov, D. Z. Albert, and L. Vaidman, Phys. Rev. Lett. **60**, 1351 (1988).
[12] N. W. M. Ritchie, J. G. Story, and R. G. Hulet, Phys. Rev. Lett. **66**, 1107 (1991).